OPEN ACCESS

University of BRISTOL

Zhou, H., Lu, Y., Yu, Q., Manners, I., & Winnik, M. (2018). Monitoring Collapse of Uniform Cylindrical Brushes with a Thermoresponsive Corona in Water. *ACS Macro Letters*, *7*(2), 166-171. https://doi.org/10.1021/acsmacrolett.7b00991

Peer reviewed version

License (if available):
CC BY

Link to published version (if available):
10.1021/acsmacrolett.7b00991

Link to publication record in Explore Bristol Research
PDF-document

University of Bristol - Explore Bristol Research
General rights

Monitoring collapse of uniform cylindrical brushes with thermo-responsive corona in water

Hang Zhou[†], Yijie Lu[†], Qing Yu[†], Ian Manners[‡], Mitchell A. Winnik[*†]

[†]Department of Chemistry, University of Toronto, Toronto, Ontario M5S 3H6, Canada
[‡]School of Chemistry, University of Bristol, Bristol BS8 1TS, United Kingdom

[*]To whom correspondence should be addressed: mwinnik@chem.utoronto.ca

ABSTRACT

We generated rod-like micelles of uniform length by living crystallization-driven self-assembly of a polyferrocenylsilane (PFS) block copolymer PFS_{26}-b-$POEGMA_{163}$ in a methanol-ethanol mixture and then transferred these micelles to water. The corona chains consisted of poly(oligoethyleneglycol methacrylate) that had a lower critical solution temperature (LCST) of 40.5 °C in water. We used a combination of static (SLS) and dynamic (DLS) multiangle light scattering to determine the dimensions of these cylindrical brush micelles in solution. Measurements carried out in dilute solution in water over a series of temperatures from 23 to 50 °C showed that the collapse transition was broad and continuous, both upon heating and cooling. This response is different from the collapse transition of $POEGMA_{163}$ homopolymer in water, which occurs over a very narrow temperature range. Thus we show that the collapse transition of a cylindrical brush has important features in common with the collapse of a brush of thermoresponsive polymers on a planar surface.

Polymer chains tethered to an impermeable surface at relatively high chain density tend to stretch away from the interface to minimize overlap, forming a polymer *brush*.[1] Many theoretical models have been developed to investigate chain conformations in the brush regime[2] and stabilization of colloidal dispersions.[3] Alexander[4] and de Gennes[5] used a scaling approach to describe a polymer brush on a planar surface. They related the thickness of the brush H to the grafting density σ and the chain length N, leading to the scaling laws $H \sim N\sigma^{1/3}$ in a good solvent and $H \sim N\sigma$ in a poor solvent. These scaling laws were later confirmed by Auroy and et al. using small-angle neutron-scattering techniques.[6] This was the first experiment to confirm the existence of the brush regime. A natural extension of studies of planar brushes is to examine polymers grafted onto curved surfaces, either cylinders or spheres.[7,8] In these examples, the volume accessible to the tethered chains increases as a function of the distance from the interface. There are many reports in the literature that examine polymer brushes on planar or spherical surfaces by different techniques.[9–14] When the tethered polymers can respond in a predicable way to specific environmental changes, these "smart" brushes find numerous uses in applications such as actuation[15], drug delivery[16], membrane separation[17], and bio-antifouling.[18] In contrast, there are many fewer examples of polymer brushes on cylindrical surfaces, and examples of cylindrical brushes of controlled length are particularly rare.[19,20] These examples consist of block copolymer (BCP) micelles and are normally characterized by a broad distribution of micelle lengths.

In this communication, we report the preparation of well-defined, water-dispersible cylindrical micelles of controlled length bearing thermo-responsive brushes. These cylindrical brushes are prepared by crystallization-driven self-assembly (CDSA)[21–23] of a crystalline-coil block copolymer poly(ferrocenyldimethylsilane)-*b*-poly(oligoethyleneglycol methyl ether methacrylate) (PFS-*b*-POEGMA). By combining multi-angle static and dynamic light scattering measurements, we studied in real time the collapse and re-swelling of the grafted POEGMA brushes in water in dilute solution (ca. 1 mg/L). The result shows for the first time, that cylindrical brushes undergo a continuous collapse upon heating and a continuous swelling upon cooling, in contrast with the sharp coil-to-globule transition of free POEGMA chains.

The polymer employed here, PFS$_{26}$-*b*-POEGMA$_{163}$ (where the subscripts refer to the mean number of repeat units), was synthesized by Click coupling of an alkyne-terminated PFS$_{26}$ and azide-terminated POEGMA$_{163}$ (see Supporting Information, SI, and Figure S1-S4 for details).

POEGMA[24,25] in water has been extensively studied as an attractive thermoresponsive alternative to Poly(N-isopropylacrylamide) (PNIPAM) due to its biocompatibility and reversible phase transition. The LCST of POEGMA can be precisely adjusted between 26 to 90 $^{\circ}$C by varying the co-monomer ratio of 2-(2-methoxyethoxy)ethyl methacrylate (MEO$_2$MA, n = 2) and oligo(ethylene glycol) methacrylate (OEGMA, n = 9). Here we synthesized an azide-terminated POEGMA possessing about 10% of OEGMA units per chain (LCST ~ 40 $^{\circ}$C) as shown in Scheme S1. The characteristics of the polymers are presented in Table S1.

Living CDSA of PFS BCPs is an effective way to prepare highly uniform rod-like micelles of controlled length.[26–28] This approach starts with the formation of long fiber-like micelles in a selective solvent that are then sonicated to form short fragments. These fragments act as seeds to initiate epitaxial growth when a solution of BCP (unimers) in a common good solvent like THF is added to the seed suspension.

Our goal was to prepare uniform cylindrical brushes of PFS$_{26}$-b-POEGMA$_{163}$ micelles in water. We began by seeking self-assembly conditions to obtain long micelles. This proved to be very challenging. All attempts at self-assembly in water failed, likely a consequence of high hydrophobicity of PFS. We have encountered this problem in the past, and, based on past experience, we examined self-assembly in water-miscible alcohol solvents with the idea of subsequently transferring the uniform micelle samples to water.[29] This approach also proved to be problematic. Heating samples of PFS$_{26}$-b-POEGMA$_{163}$ in methanol or ethanol (or in their mixtures) led to short cylindrical micelles (ca. 80 nm long) accompanied by small spherical micelles. We have previously reported the co-existence of spherical and rod-like micelles in alcohol media for other PFS BCP systems including PFS-b-P2VP (poly-2-vinylpyridine)[30] and PFS-b-PNIPAM (poly-N-isopropylacrylamide).[31] In those examples, the rod micelles had a semi-crystalline PFS core, whereas the spherical micelles were amorphous. Here, the PFS$_{26}$-b-POEGMA$_{163}$ micelles in ethanol aggregated to form a stacked layer on the TEM grid. Similar experiments in 2-propanol gave a precipitate. More details are presented in SI. Lowe[32] and Theato[33] have reported that POEGMA exhibits an upper critical solution temperature (UCST) in many aliphatic alcohols. The UCST was found to increase with increasing concentration and carbon number of the solvent. This finding explains why this BCP in ethanol and in 2-propanol tends to aggregate and precipitate, whereas it forms clear solutions of stable micelles in methanol.

We then modified the self-assembly protocol, adding a solution of PFS$_{26}$-b-POEGMA$_{163}$ in minimal amount of THF (ca. 5 μL) to an excess of hot methanol or ethanol (2 mL), followed by heating and cooling. The sample in methanol gave a clear solution, whereas the sample in ethanol was turbid. Here the TEM images were different. As shown in Figure S5 panel D and E, narrow lenticular platelets several micrometers long were found in methanol while large aggregates of fiber-like micelles had formed in ethanol. No spherical micelles were detected in in either sample, suggesting that all of the PFS BCP molecules were incorporated in the crystalline core of these objects. Based on these results, we added the THF solution of PFS$_{26}$-b-POEGMA$_{163}$ to methanol:ethanol mixtures. For a 1:4 volume ratio, we obtained a clear solution of long (> 10 μm) fiber-like micelles (Figure S5F). This sample was then subjected to sonication (30 min, 23 °C, 70 watt ultrasonic cleaning bath), forming short rod-like micelle fragments (L_n = 64.7 nm, L_w = 74.1 nm, L_w/L_n = 1.15). Here L_n and L_w are the number- and weight-average micelle lengths.
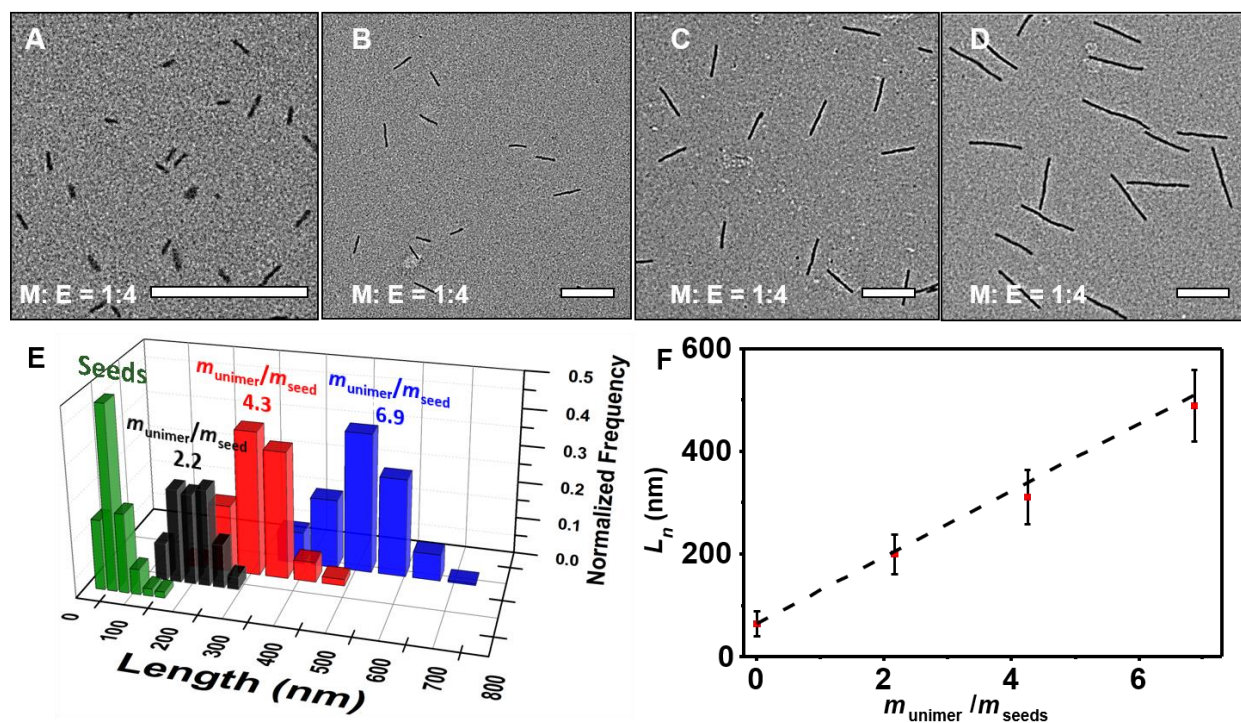

Figure 1. TEM images of PFS$_{26}$-b-POEGMA$_{163}$ micelles prepared by seeded growth in a mixed solvent of methanol:ethanol (1:4 v/v). (A) Seed micelles generated by sonication of fiber-like micelles prepared in this mixed solvent. (B-D) Uniform cylindrical micelles of different lengths obtained by adding different amounts of PFS$_{26}$-b-POEGMA$_{163}$ unimers in THF to a suspension of the seed micelles. (E) Length histograms of the micelles shown in parts A-D. (F) Number average length L_n versus m_{unimer}/m_{seed} for the micelles shown in parts A-D The dashed line represents the predicted lengths based on eq. S2 assuming that all added unimer has added to the seed micelles. Scale bars: 500 nm.

Seeded growth experiments were carried out by adding different amounts of PFS$_{26}$-b-POEGMA$_{163}$ (40 µg, 100 µg, 200 µg) as a 20 mg/mL solution in THF to separate vials containing 20 µg (0.01 mg/mL, 2 mL) seed micelles in 1:4 methanol:ethanol, followed by aging for at least a week at room temperature. Linear rod-like micelles of narrow length distribution (Figure 1) were obtained. Values of L_n increased with the unimer/seed ratio as predicted (eq. S2, Figure 1F) by a model that assumes that all of the added unimer grew epitaxially on the ends of the seed micelles. In this way we obtained a family of rod-like micelles with excellent control over their length.
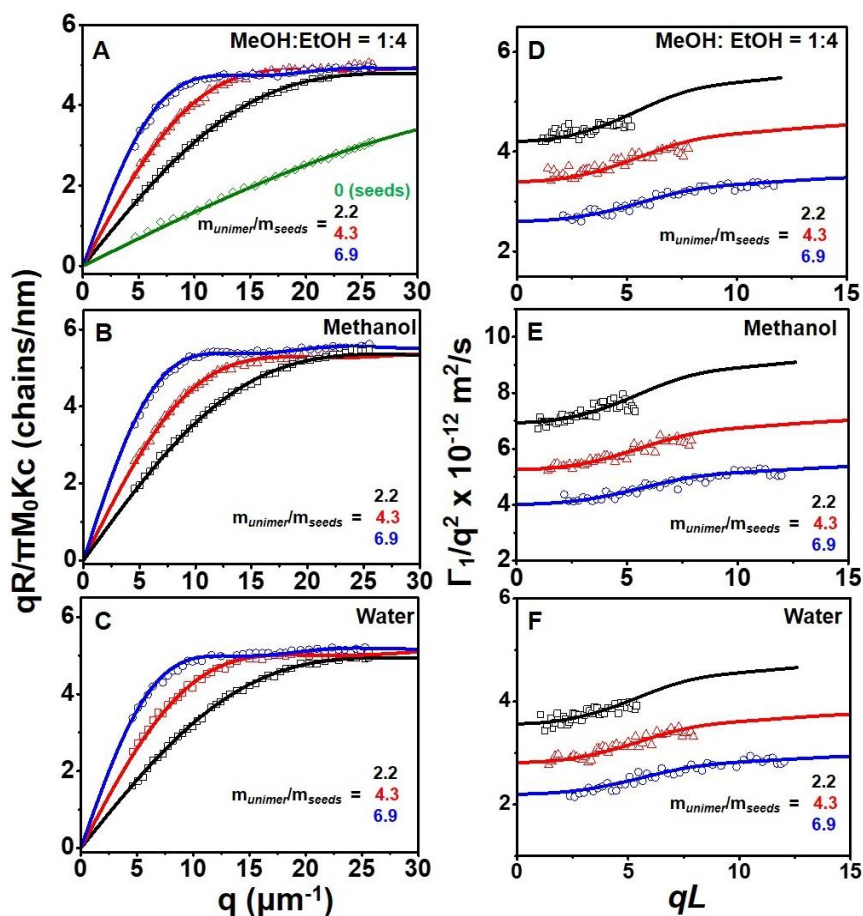

Figure 2. SLS (Holtzer-Casassa plots of $qR_\theta/\pi M_0 Kc$ as a function of q, A-C) and DLS (Plots of Γ_1/q_2 as a function of qL, where L corresponds to SLS L_w values) for uniform PFS$_{26}$-b-POEGMA$_{163}$ micelles dispersed in methanol/ethanol (1:4 v/v, A, D), methanol (B, E) and water (C, F). The different color data points refer to micelles formed at different unimer-to-seed ratios (m_{unimer}/m_{seed}). Each line represents the best fit of the data to eq. S3 (SLS) or eq. S9 (DLS). The green line in A is for the initial seed micelles used for CDSA of the longer rod-like micelles.

The next challenge was to transfer the micelles to methanol and to water in order to investigate their properties. In the past, we had difficulty transferring PFS$_{26}$-b-PNIPAM$_{520}$

micelles from 2-propanol to water. Various transfer protocols led to fragmentation of the micelles, which we attributed to the co-nonsolvency effect of alcohol-water mixtures on the PNIPAM chains.[31] Here we report that simple injection of PFS_{26}-b-$POEGMA_{163}$ micelle solutions (40 µL) into excess water or methanol (1 mL) led to successful transfer. As shown in the TEM images and histograms in Figure S7 as well as in the comparative data in Table S3, all the micelle samples retained their lengths and narrow size distributions after the transfer. In the analysis of these samples described below, we ignore the tiny amounts of methanol or ethanol in the final solutions.

Table 1. Summary of structural parameters characterized by TEM and light scattering of micelles in different solvents [a]

Solvent	m_{unimer}/m_{seed}	$L_{w,\,TEM}$ (nm)	$L_{w,\,SLS}$ (nm)	$N_{agg,L}$ (chains/nm)	R_{SLS} (nm)	R_{DLS} (nm)
	seeds	74	78	5.5	16	-
MeOH/EtOH (v:v = 1:4)	2.0	208	200	5.4	10	22
	4.6	321	300	5.3	10	22
	7.3	510	450	5.3	10	23
MeOH	2.0	204	210	6.0	10	21
	4.6	325	310	5.9	10	22
	7.3	475	470	6.0	10	24
Water	2.0	207	210	5.6	10	27
	4.6	306	310	5.6	10	28
	7.3	484	470	5.6	10	28

[a.] Seeded growth in methanol:ethanol = 1:4 v/v followed by transfer to methanol or water.

Each of these dilute micelle solutions (ca. 1 µg/mL, in water, methanol and methanol:ethanol 1:4 v/v) was examined by multiangle SLS and DLS measurements. The SLS data are presented as Holtzer-Casassa (HC) plots (Figure 2A, B, and C) of $qR_\theta/\pi M_0 Kc$ as a function of q (eq. S3). The parameters R_θ, the Rayleigh ratio, q, the scattering vector, and the optical constant K are defined in SI. M_0 is the molecular weight of the BCP. Three important parameters are determined from the fitting of these plots: (i) L_w, (ii) the number of block copolymer per unit length of the micelles, a value we refer as the linear aggregation number,

$N_{agg/L}$ and (iii) the radius of the cylinder cross section, R_{SLS}.[31,34,35] The DLS data (Figure 2D, E, F) are analyzed in terms of a model derived by Wilcoxon and Schurr[36] (eq. S9), from which we calculate the hydrodynamic radius cross section, R_{DLS}. In rod-like micelles, R_{SLS} is fundamentally different and always smaller than R_{DLS}. R_{SLS} accounts for the mass distribution of the scattering object, which is dominated by the dense micelle core and the higher density of corona chains near the micelle surface. In contrast, the corona chains that extend far from the micelle surface provide hydrodynamic resistance to diffusion and contribute to the magnitude of R_{DLS}. All the fitting parameters are summarized in Table 1. From this table, we see that L_w values from TEM images and from the HC plots are in excellent agreement with each other, which provides confidence in our data analysis. Values of $N_{agg/L}$ (5.5~6 chains/nm) and R_{SLS} (10 nm) are essentially identical not only for samples prepared at different m_{unimer}/m_{seed} ratios, but also for samples transferred to different solvents. The consistent values of $N_{agg/L}$ for micelle samples in different solvents indicates that transfer of the micelles to water and to methanol did not affect the structure of the micelles. The high value of $N_{agg/L}$ suggests that the packing is quite dense in the semicrystalline micelle core.

Analysis of the DLS data led to values of R_{DLS} = 22 nm in both alcoholic media and R_{DLS} = 28 nm in water (as shown in Table 1). These differences between water and alcohol solvents indicate that POEGMA is somewhat more swollen in water than in methanol or 1:4 methanol:ethanol.

One micelle sample with L_w = 210 nm (m_{unimer}/m_{seed} = 2.2, Figure S7 panel E) was chosen for a careful study of the thermal response of the micelles in water. These experiments were conducted in very dilute solution (1 µg/mL) to avoid inter-micellar aggregation. This sample was heated from 23 to 50 °C and then cooled. SLS and DLS measurements were carried out after equilibration for 30 min at each temperature, and a Zimm analysis provided values of the weight-averaged molecular weight (M_w) and the radius of gyration ($<R_g^2>^{1/2}$) of the micelles. In Figure 3A we show that the values of M_w and $<R_g^2>^{1/2}$ do not change during the heating and cooling cycle; thus the micelles remain intact,[37] and no aggregation could be detected. As a check on these measurements, we calculated the apparent length of the micelles L from eq. 1, based on the model of a rigid rod. Using the measured values of $<R_g^2>^{1/2}$ = 65 nm and $R = R_{SLS}$ = 10 nm, this calculation yielded L = 224 nm, consistent with the value of L_w = 210 nm obtained by TEM and from the HC plot.

$$\langle R_g^2 \rangle = \frac{R^2}{2} + \frac{L^2}{12} \tag{1}$$

Figure 3B shows the temperature dependence of the cross section hydrodynamic radius (R_{DLS}) in one heating-and-cooling cycle. One can see that R_{DLS} changes continuously from 26.5 nm at 30 °C to 19 nm at 50 °C, with the corona chains shrinking during the heating process and re-swelling in the cooling process. This continuous collapse of POEGMA polymer brush grafted on cylindrical surface is markedly different from the sharp coil-to-globule transition of individual POEGMA chain free in water. The LCST of POEGMA homopolymer used in our experiment is 40.5 °C (Figure S8A) at concentrations high enough (5 mg/mL) to visualize the cloud point, or at ca. 43 °C (Figure S8B) in dilute solution (0.3 mg/mL) as determined by light scattering. We picture the collapse transition of the micelle corona in Scheme 1.
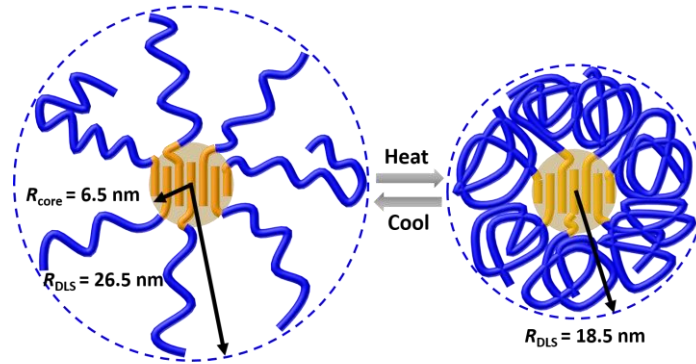
Scheme 1. A representation in cross section of the thermally induced collapse of the cylindrical polymer brush of the corona chains of PFS$_{26}$-*b*-POEGMA$_{163}$ micelles in water.

To gain a better understanding of the continuous collapse transition, we calculated the surface grafting density (σ) of POEGMA chains to the PFS core. The value of σ can be evaluated (eq. 2) as the ratio of $N_{agg/L}$ (determined by SLS) to the circumference of the cylinder[38] (estimated from the mean width of the micelle core ($W_{core} \approx 13$ nm) in TEM images, Figure S9).

$$\sigma = \frac{N_{agg/L}}{\pi W_{core}} \tag{2}$$

In this way, we calculate a value of $\sigma = 0.12$ chains/nm^2, which corresponds to an average grafting-point distance of ca. 3 nm. This value is much smaller than the $\langle R_g^2 \rangle^{1/2}$ of the corona chains (ca. 7.2 nm), which we calculated as $1.5 \times R_h$ for POEGMA$_{163}$ homopolymer in water (4.8 nm, CONTIN plot in Figure S8B), indicating overcrowding of tethered POEGMA chains. The magnitude of the reduced tethered chain density $\tilde{\sigma} = \sigma\pi\langle R_g^2\rangle$[39] is a more quantitative measure of overcrowding. Here we find a value of $\tilde{\sigma} = 19.5$, much larger than 14.3, which represents the

9

onset of the highly stretched brush regime.[40] Based on a model proposed by Wu,[41] we used the grafting density to estimate a mean free energy of 14.6 kT per grafted chain (details are provided in SI), also consistent with a highly stretched brush. Previously, Halperin and co-workers[42] proposed a two-state model to depict the phase behavior of polymer brushes based on self-consistent field theory. In this model, the collapse first occurs at the bottom of the swollen brush with higher monomer concentration, and then progresses toward its external dilute surface as the solvent quality decreases. A continuous collapse transition over a relatively wide range of temperatures has been reported several times for planar brushes with thermo-responsive polymers like PNIPAM[43–45] and POEGMA.[46] Our experiments further extend this behavior to a thermoresponsive polymer brush on a cylindrical surface.
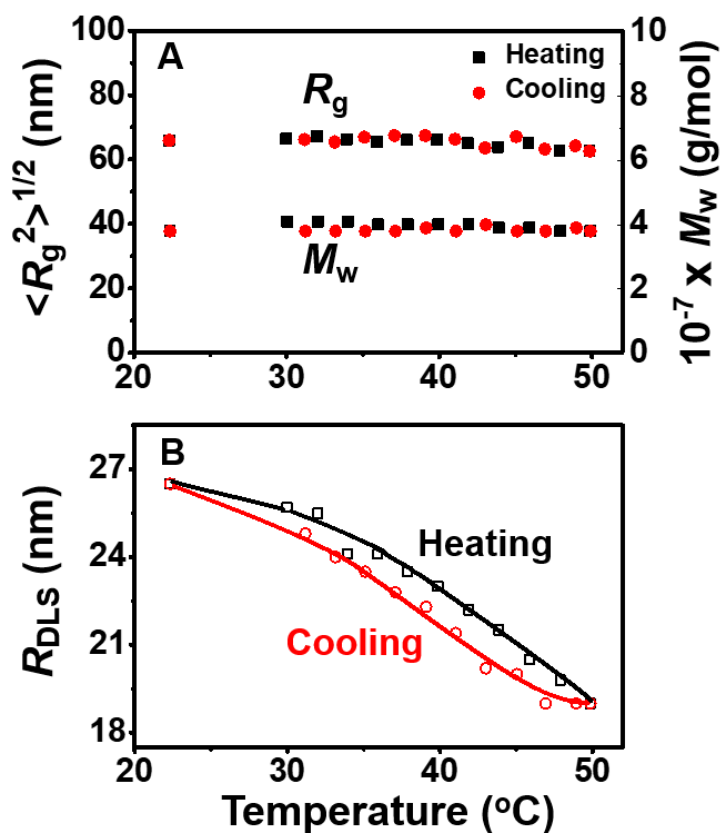

Figure 3. (A) Radius of gyration $\langle R_g^2 \rangle^{1/2}$ and weight-averaged molecular weight (M_w) of PFS$_{26}$-b-POEGMA$_{163}$ micelles characterized by SLS during the heating and cooling cycle. (B) Hydrodynamic radius of the cross section (R_{DLS}) over the same temperature range.

In conclusion, we prepared thermo-responsive cylindrical polymer brushes in water consisting of uniform rod-like PFS$_{26}$-b-POEMGA$_{163}$ BCP micelles, whose length could be controlled via living CDSA. Multiangle SLS and DLS measurements showed that the corona

chains tethered to the micelle core were in the stretched brush regime. Experiments carried out over a temperature range of 23 - 50 ºC showed a continuous collapse of the corona chains upon heating and a continuous re-swelling upon cooling, rather than a sharp critical solubility transition characteristic of the POEMGA homopolymer in water. Currently we are examining potential biomedical applications of these aqueous rod-like micelles.

ASSOCIATED CONTENT

Supporting Information. Experimental details and characterization data (NMR, GPC, SLS, DLS, TEM), light scattering data analysis method, and additional results and discussion. This material is available free of charge via the Internet at http://pubs.acs.org.

ACKNOWLEDGMENTS

REFERENCES

(1)   Milner, S. T. Polymer Brushes. *Science* **1991**, *251*, 905–914.

(2)   Gerle, M.; Fischer, K.; Roos, S.; Müller, A. H. E.; Schmidt, M.; Sheiko, S. S.; Prokhorova, S.; Möller, M. Main Chain Conformation and Anomalous Elution Behavior of Cylindrical Brushes As Revealed by GPC/MALLS, Light Scattering, and SFM. *Macromolecules* **1999**, *32*, 2629–2637.

(3)   Zhulina, E. B.; Borisov, O. V.; Priamitsyn, V. A. Theory of Steric Stabilization of Colloid Dispersions by Grafted Polymers. *J. Colloid Interface Sci.* **1990**, *137*, 495–511.

(4)   Alexander, S. Adsorption of Chain Molecules with a Polar Head a Scaling Description. *J. Phys.* **1977**, *38*, 983–987.

(5)   de Gennes, P. G. Conformations of Polymers Attached to an Interface. *Macromolecules* **1980**, *13*, 1069–1075.

(6)   Auroy, P.; Auvray, L.; Léger, L. Characterization of the Brush Regime for Grafted Polymer Layers at the Solid-Liquid Interface. *Phys. Rev. Lett.* **1991**, *66*, 719–722.

(7)   Wijmans, C. M.; Zhulina, E. B. Polymer Brushes at Curved Surfaces. *Macromolecules* **1993**, *26*, 7214–7224.

(8)   Murat, M.; Grest, G. S. Polymers End-Grafted onto a Cylindrical Surface. *Macromolecules* **1991**, *24*, 704–708.

(9)   Zhou, T.; Qi, H.; Han, L.; Barbash, D.; Li, C. Y. Towards Controlled Polymer Brushes via a Self-Assembly-Assisted-Grafting-to Approach. *Nat. Commun.* **2016**, *7*, ncomms11119.

(10)   Srivastava, S.; Agarwal, P.; Archer, L. A. Tethered Nanoparticle–Polymer Composites: Phase Stability and Curvature. *Langmuir* **2012**, *28*, 6276–6281.

(11)   Karim, A.; Satija, S. K.; Douglas, J. F.; Ankner, J. F.; Fetters, L. J. Neutron Reflectivity Study of the Density Profile of a Model End-Grafted Polymer Brush: Influence of Solvent Quality. *Phys. Rev. Lett.* **1994**, *73*, 3407–3410.

(12)   Wu, T.; Zhang, Y.; Wang, X.; Liu, S. Fabrication of Hybrid Silica Nanoparticles Densely Grafted with Thermoresponsive Poly(N-Isopropylacrylamide) Brushes of Controlled Thickness via Surface-Initiated Atom Transfer Radical Polymerization. *Chem. Mater.* **2008**, *20*, 101–109.

(13)   Xu, J.; Luo, S.; Shi, W.; Liu, S. Two-Stage Collapse of Unimolecular Micelles with Double Thermoresponsive Coronas. *Langmuir* **2006**, *22*, 989–997.

(14)   Xu, W.; Choi, I.; Plamper, F. A.; Synatschke, C. V.; Müller, A. H. E.; Melnichenko, Y. B.; Tsukruk, V. V. Thermo-Induced Limited Aggregation of Responsive Star Polyelectrolytes. *Macromolecules* **2014**, *47*, 2112–2121.

(15)   Zhou, F.; Shu, W.; Welland, M. E.; Huck, W. T. S. Highly Reversible and Multi-Stage Cantilever Actuation Driven by Polyelectrolyte Brushes. *J. Am. Chem. Soc.* **2006**, *128*, 5326–5327.

(16)   Kataoka, K.; Harada, A.; Nagasaki, Y. Block Copolymer Micelles for Drug Delivery: Design, Characterization and Biological Significance. *Adv. Drug Deliv. Rev.* **2012**, *64*, 37–48.

(17)   Keating, J. J.; Imbrogno, J.; Belfort, G. Polymer Brushes for Membrane Separations: A Review. *ACS Appl. Mater. Interfaces* **2016**, *8*, 28383–28399.

(18)   Yang, W. J.; Neoh, K.-G.; Kang, E.-T.; Teo, S. L.-M.; Rittschof, D. Polymer Brush Coatings for Combating Marine Biofouling. *Prog. Polym. Sci.* **2014**, *39*, 1017–1042.

(19)   Blanazs, A.; Verber, R.; Mykhaylyk, O. O.; Ryan, A. J.; Heath, J. Z.; Douglas, C. W. I.; Armes, S. P. Sterilizable Gels from Thermoresponsive Block Copolymer Worms. *J. Am. Chem. Soc.* **2012**, *134*, 9741–9748.

(20)   Qian, J.; Zhang, M.; Manners, I.; Winnik, M. A. Nanofiber Micelles from the Self-Assembly of Block Copolymers. *Trends Biotechnol.* **2010**, *28*, 84–92.

(21) Tritschler, U.; Pearce, S.; Gwyther, J.; Whittell, G. R.; Manners, I. 50th Anniversary Perspective: Functional Nanoparticles from the Solution Self-Assembly of Block Copolymers. *Macromolecules* **2017**, *50*, 3439–3463.

(22) Hailes, R. L. N.; Oliver, A. M.; Gwyther, J.; Whittell, G. R.; Manners, I. Polyferrocenylsilanes: Synthesis, Properties, and Applications. *Chem. Soc. Rev.* **2016**, *45*, 5358–5407.

(23) He, W.-N.; Xu, J.-T. Crystallization Assisted Self-Assembly of Semicrystalline Block Copolymers. *Prog. Polym. Sci.* **2012**, *37*, 1350–1400.

(24) Lutz, J.-F.; Hoth, A. Preparation of Ideal PEG Analogues with a Tunable Thermosensitivity by Controlled Radical Copolymerization of 2-(2-Methoxyethoxy)ethyl Methacrylate and Oligo(ethylene Glycol) Methacrylate. *Macromolecules* **2006**, *39*, 893–896.

(25) Lutz, J.-F.; Akdemir, Ö.; Hoth, A. Point by Point Comparison of Two Thermosensitive Polymers Exhibiting a Similar LCST: Is the Age of Poly(NIPAM) Over? *J. Am. Chem. Soc.* **2006**, *128*, 13046–13047.

(26) Gilroy, J. B.; Gädt, T.; Whittell, G. R.; Chabanne, L.; Mitchels, J. M.; Richardson, R. M.; Winnik, M. A.; Manners, I. Monodisperse Cylindrical Micelles by Crystallization-Driven Living Self-Assembly. *Nat. Chem.* **2010**, *2*, 566–570.

(27) Wang, X.; Guerin, G.; Wang, H.; Wang, Y.; Manners, I.; Winnik, M. A. Cylindrical Block Copolymer Micelles and Co-Micelles of Controlled Length and Architecture. *Science* **2007**, *317*, 644–647.

(28) Gädt, T.; Ieong, N.; Cambridge, G.; Winnik, M.; Manners, I. Complex and Hierarchical Micelle Architectures from Diblock Copolymers Using Living, Crystallization-Driven Polymerizations. *Nat. Mater.* **2009**, *8*, 144–150.

(29) Nazemi, A.; Boott, C. E.; Lunn, D. J.; Gwyther, J.; Hayward, D. W.; Richardson, R. M.; Winnik, M. A.; Manners, I. Monodisperse Cylindrical Micelles and Block Comicelles of Controlled Length in Aqueous Media. *J. Am. Chem. Soc.* **2016**, *138*, 4484–4493.

(30) Shen, L.; Wang, H.; Guerin, G.; Wu, C.; Manners, I.; Winnik, M. A. A Micellar Sphere-to-Cylinder Transition of Poly(ferrocenyldimethylsilane-*b*-2-Vinylpyridine) in a Selective Solvent Driven by Crystallization. *Macromolecules* **2008**, *41*, 4380–4389.

13

(31) Zhou, H.; Lu, Y.; Zhang, M.; Guerin, G.; Manners, I.; Winnik, M. A. PFS-*b*-PNIPAM: A First Step toward Polymeric Nanofibrillar Hydrogels Based on Uniform Fiber-Like Micelles. *Macromolecules* **2016**, *49*, 4265–4276.

(32) Roth, P. J.; Davis, T. P.; Lowe, A. B. Comparison between the LCST and UCST Transitions of Double Thermoresponsive Diblock Copolymers: Insights into the Behavior of POEGMA in Alcohols. *Macromolecules* **2012**, *45*, 3221–3230.

(33) J. Roth, P.; D. Jochum, F.; Theato, P. UCST-Type Behavior of Poly[oligo(ethylene Glycol) Methyl Ether Methacrylate] (POEGMA) in Aliphatic Alcohols : Solvent , Co-Solvent, Molecular Weight, and End Group Dependences. *Soft Matter* **2011**, *7*, 2484–2492.

(34) Guerin, G.; Qi, F.; Cambridge, G.; Manners, I.; Winnik, M. A. Evaluation of the Cross Section of Elongated Micelles by Static and Dynamic Light Scattering. *J. Phys. Chem. B* **2012**, *116*, 4328–4337.

(35) Zhou, H.; Lu, Y.; Qiu, H.; Guerin, G.; Manners, I.; Winnik, M. A. Photocleavage of the Corona Chains of Rigid-Rod Block Copolymer Micelles. *Macromolecules* **2015**, *48*, 2254–2262.

(36) Wilcoxon, J.; Schurr, J. M. Dynamic Light Scattering from Thin Rigid Rods: Anisotropy of Translational Diffusion of Tobacco Mosaic Virus. *Biopolymers* **1983**, *22*, 849–867.

(37) Qian, J.; Lu, Y.; Cambridge, G.; Guerin, G.; Manners, I.; Winnik, M. A. Polyferrocenylsilane Crystals in Nanoconfinement: Fragmentation, Dissolution, and Regrowth of Cylindrical Block Copolymer Micelles with a Crystalline Core. *Macromolecules* **2012**, *45*, 8363–8372.

(38) Guerin, G.; Rupar, P.; Molev, G.; Manners, I.; Jinnai, H.; Winnik, M. A. Lateral Growth of 1D Core-Crystalline Micelles upon Annealing in Solution. *Macromolecules* **2016**, *49*, 7004–7014.

(39) Chen, W. Y.; Zheng, J. X.; Cheng, S. Z. D.; Li, C. Y.; Huang, P.; Zhu, L.; Xiong, H.; Ge, Q.; Guo, Y.; Quirk, R. P.; Lotz, B.; Deng, L.; Wu, C.; Thomas, E. L.Onset of Tethered Chain Overcrowding. *Phys. Rev. Lett.* **2004**, *93*, 028301.

(40) Zheng, J. X.; Xiong, H.; Chen, W. Y.; Lee, K.; Van Horn, R. M.; Quirk, R. P.; Lotz, B.; Thomas, E. L.; Shi, A.-C.; Cheng, S. Z. D. Onsets of Tethered Chain Overcrowding and Highly Stretched Brush Regime via Crystalline−Amorphous Diblock Copolymers. *Macromolecules* **2006**, *39*, 641–650.

(41)   Wu, C. How Does a Polymer Brush Repel Proteins? *Chin. J. Polym. Sci.* **2014**, *32*, 1575–1580.

(42)   Baulin, V. A.; Zhulina, E. B.; Halperin, A. Self-Consistent Field Theory of Brushes of Neutral Water-Soluble Polymers. *J. Chem. Phys.* **2003**, *119*, 10977–10988.

(43)   Liu, G.; Zhang, G. Collapse and Swelling of Thermally Sensitive Poly(N-Isopropylacrylamide) Brushes Monitored with a Quartz Crystal Microbalance. *J. Phys. Chem. B* **2005**, *109*, 743–747.

(44)   Zhang, G. Study on Conformation Change of Thermally Sensitive Linear Grafted Poly(N-Isopropylacrylamide) Chains by Quartz Crystal Microbalance. *Macromolecules* **2004**, *37*, 6553–6557.

(45)   Montagne, F.; Polesel-Maris, J.; Pugin, R.; Heinzelmann, H. Poly(N-Isopropylacrylamide) Thin Films Densely Grafted onto Gold Surface: Preparation, Characterization, and Dynamic AFM Study of Temperature-Induced Chain Conformational Changes. *Langmuir* **2009**, *25*, 983–991.

(46)   Laloyaux, X.; Mathy, B.; Nysten, B.; Jonas, A. M. Surface and Bulk Collapse Transitions of Thermoresponsive Polymer Brushes. *Langmuir* **2010**, *26*, 838–847.

For Table of Contents Only:

TOC:

Uniform PFS$_{26}$-*b*-POEGMA$_{163}$ cylinders in water

Heat

Cool
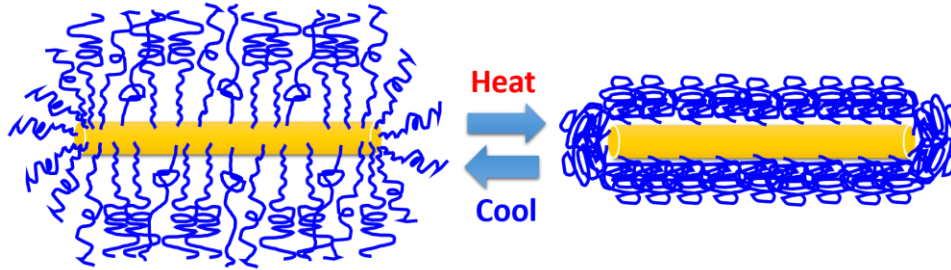
Continuous collapse of polymer brushes on cylindrical surface